

A DISCRETE COLLOCATION METHOD FOR BOUNDARY INTEGRAL EQUATIONS

YAJUN YANG

ABSTRACT. We propose a discrete collocation method for the boundary integral equations which arise from solving Laplace's equation $\Delta u = 0$. The Laplace's equation is defined on connected regions D in \mathbf{R}^3 with a smooth boundary S . The piecewise polynomial interpolation in the parametrization variables along with the collocation method is used, and a numerical integration scheme for collocation integrals is given. We give an estimation on the rate of convergence and present some numerical examples for the exterior Neumann problem.

1. Introduction. We propose a discrete collocation method for the boundary integral equations of the second kind for solving Laplace's equation $\Delta u = 0$ on connected regions D in \mathbf{R}^3 . The integral equations we considered have the following form:

$$(1.1) \quad 2\pi\rho(P) + \int_S \rho(Q) \frac{\partial}{\partial\nu_Q} \left[\frac{1}{|P-Q|} \right] dS_Q = g(P), \quad P \in S.$$

Symbolically, we rewrite the integral equation (1.1) as

$$(2\pi + \mathcal{K})\rho = g$$

where $\mathcal{K} : C(S) \rightarrow C(S)$ defined by

$$\mathcal{K}\rho(P) = \int_S \rho(Q) \frac{\partial}{\partial\nu_Q} \left[\frac{1}{|P-Q|} \right] dS_Q$$

is a bounded compact linear operator.

To see where the above integral equations may arise in solving Laplace's equation, consider the following two problems:

Received by the editors on March 7, 1994, and in revised form on January 25, 1995.

Key words. Numerical integration, quadratic interpolation, adaptive refinement, collocation method.

AMS MOS *Subject Classification.* 65D30, 65D32, 65R20.

Copyright ©1995 Rocky Mountain Mathematics Consortium

A. *The interior Dirichlet problem.* Let D be a bounded, open, simply connected region in \mathbf{R}^3 , and let its boundary S be smooth, which is defined more precisely in Section 2. The problem is to find $u \in C(\overline{D}) \cap C^2(D)$ such that

$$\begin{aligned}\Delta u(A) &= 0, & A \in D \\ u(P) &= f(P), & P \in S.\end{aligned}$$

We assume that u can be represented as a double layer potential:

$$(1.2) \quad u(A) = \int_S \rho(Q) \frac{\partial}{\partial \nu_Q} \left[\frac{1}{|A-Q|} \right] dS_Q, \quad A \in D.$$

The density function ρ is determined from the integral equation

$$(1.3) \quad 2\pi\rho(P) + \int_S \rho(Q) \frac{\partial}{\partial \nu_Q} \left[\frac{1}{|P-Q|} \right] dS_Q = f(P), \quad P \in S.$$

For notation, ν_Q denotes the unit normal to S at Q (if it exists), pointing into D .

B. *The exterior Neumann problem.* Let D and S be as above, and let $D_e = \mathbf{R}^3 \setminus \overline{D}$, the region exterior to D and S . The problem is to find $u \in C(\overline{D}_e) \cap C^2(D_e)$ such that

$$(1.4) \quad \begin{aligned}\Delta u(A) &= 0, & A \in D_e \\ \frac{\partial u(P)}{\partial \nu_P} &= f(P), & P \in S \\ u(P) &= O(|P|^{-1}), & |\nabla u(P)| = O(|P|^{-2}) \\ & & \text{as } |P| \rightarrow \infty.\end{aligned}$$

It can be shown that such a function u exists (under suitable assumptions on S and f) and that Green's third identity can be applied to u :

$$(1.5) \quad 4\pi u(A) = \int_S f(Q) \frac{1}{|A-Q|} dS_Q - \int_S u(Q) \frac{\partial}{\partial \nu_Q} \left[\frac{1}{|A-Q|} \right] dS_Q, \quad A \in D_e.$$

To find u on S , we solve the integral equation

$$(1.6) \quad 2\pi u(P) + \int_S u(Q) \frac{\partial}{\partial \nu_Q} \left[\frac{1}{|P-Q|} \right] dS_Q = \int_S f(Q) \frac{1}{|P-Q|} dS_Q, \quad P \in S.$$

Then (1.5) gives u on D_e . The integral equation (1.6) is of the form (1.1) with

$$g = \int_S f(Q) \frac{1}{|P-Q|} dS_Q \equiv \mathcal{S}f.$$

\mathcal{S} is the single layer potential integral operator.

The collocation method has been used with piecewise polynomial approximations to solve (1.1) and problems arising in potential theory. Piecewise constant collocation has been discussed by Jaswon and Symm [15], Lynn and Timlake [20], and others. The piecewise quadratic method is analyzed by Atkinson [2, 3] and Wait [25]. A simple framework for the analysis of collocation methods that use piecewise polynomial interpolation is also presented in [2]. The most general convergence results for collocation methods are given by Wendland [26]. He used polynomials of degree k to approximate surfaces and polynomials of degree d to approximate functions, and he showed that the error of the numerical solution is of order n , where n is the minimum of $d + 1$ and $k + 1$. The superconvergence result for the collocation method with piecewise quadratic approximations for both the surface S and the unknown solution ρ was obtained by Atkinson and Chien [8].

The key to the implementation of the collocation method is the numerical quadratures for the collocation integrals. For the boundary integral equations we considered in (1.1), there are no straightforward quadrature rules available. This is simply because several different types of integrals are involved, including the singular integrals appearing in the collocation system. When the integrand has singularities within the integration region, the use of a standard quadrature method may be very inefficient. Schwab and Wendland [24] presented and analyzed methods for the accurate and efficient evaluation of weakly singular, Cauchy singular and hypersingular integrals. The approach of using extrapolation methods to construct new and more accurate integration formulas based on the asymptotic expansion for the quadrature error was discussed in Lyness [18] and [19]. Rathsfeld [22, 23] gave

numerical integration methods associated with graded meshes when numerically solving the integral equation over the boundary of a polyhedron.

Atkinson [5] and Atkinson and Chien [8] presented numerical schemes for evaluating collocation integrals. Their numerical integration methods were chosen after much experimentation with other approaches and were shown to be very efficient in the numerical examples. The collocation method described in [8] was then implemented with these schemes. The empirical convergence rate for the approximate solution of boundary integral equations is consistent with the superconvergence result for the collocation solution. However, there is no error analysis for the approximate solution. In this paper we propose a discrete collocation method by choosing a proper integration scheme and show that the superconvergence result of [8] is still valid for the approximate solution obtained by the discrete collocation method.

The rest of the paper is organized as follows. In Section 2 we describe the triangulation of the surface S and the refinement scheme we use. The interpolation-based quadrature formulas are given in Section 3. Section 4 contains the collocation method with piecewise polynomial interpolation. A discrete collocation method based on previous three sections is presented in Section 5, and numerical examples are given in Section 6.

2. The triangulation and refinement. We assume that S is a *smooth surface* in \mathbf{R}^3 . By this, we mean that for each point $P \in S$, there is a neighborhood on S of P , with the neighborhood having a local five-times continuously differentiable parametrization in \mathbf{R}^2 . We also assume that S is closed and can be written as

$$(2.1) \quad S = S_1 \cup S_2 \cup \cdots \cup S_J$$

and for each S_j there is a mapping

$$(2.2) \quad F_j : R_j \xrightarrow[\text{onto}]{1-1} S_j, \quad j = 1, \dots, J,$$

where R_j is a polygonal domain in the plane and $F_j \in C^5(R_j)$. Moreover, the only possible intersection of a pair S_i and S_j is to be either a common vertex or along a common portion of the edges of these two sub-surfaces.

The surface S of (2.1) is divided into a triangular mesh

$$(2.3) \quad \tau_n = \{\Delta_{k,n} \mid k = 1, \dots, N_n\}$$

for a sequence $n = 1, 2, \dots$. One way of obtaining the triangulation (2.3) is by means of the parametric representation (2.2) for the region S_j of (2.1). We create triangulations for S by first triangulating each R_j and then mapping this triangulation onto S_j . Since the R_j 's are polygonal domains and can be written as a union of triangles, without loss of generality, we assume in this paper that the R_j 's are triangles. We choose

$$\Delta_{k,1} = F_k(R_k) = S_k, \quad k = 1, \dots, J$$

and

$$\tau_1 = \{\Delta_{k,1} \mid k = 1, \dots, J\}.$$

The sequence of triangulations (2.3) will usually be obtained by successive refinements. Given a triangulation $\hat{\tau}_n$ at level n , and given a triangle $\hat{\Delta}_{k,n}$ in some R_j , $j = 1, \dots, J$, refine it into smaller triangles by using straight line segments to connect the midpoints of the three sides of $\hat{\Delta}_{k,n}$ (see Figure 1). The four new triangles will be congruent, and they will be similar to the original triangle $\hat{\Delta}_{k,n}$. More importantly, any *symmetric pair of triangles*, say $\hat{\Delta}_k$ and $\hat{\Delta}_l$ as shown in Figure 2, have the following property:

$$(2.4) \quad \hat{v}_{2,k} - \hat{v}_{1,k} = -(\hat{v}_{2,l} - \hat{v}_{1,l})$$

and

$$\hat{v}_{3,k} - \hat{v}_{1,k} = -(\hat{v}_{3,l} - \hat{v}_{1,l}).$$

After such a refinement of all triangles in the triangulation $\hat{\tau}_n$, we will have a new triangulation τ_{n+1} under the parametric representation (2.2) with four times the number of triangles in τ_n , i.e., $N_{n+1} = 4N_n$. And the total number of symmetric pairs of triangles in $\hat{\tau}_n$ is $O(N_n)$ and the remaining triangles in $\hat{\tau}_n$ is $O(\sqrt{N_n})$. Define the mesh size of $\hat{\tau}_n$ by

$$(2.5) \quad \begin{aligned} \hat{\delta}_n &= \max_{1 \leq k \leq N_n} \text{diam}(\hat{\Delta}_k), \\ \text{diam}(\hat{\Delta}_k) &= \max_{p, q \in \hat{\Delta}_k} |p - q| \end{aligned}$$

then $\hat{\delta}_{n+1} = \hat{\delta}_n/2$.

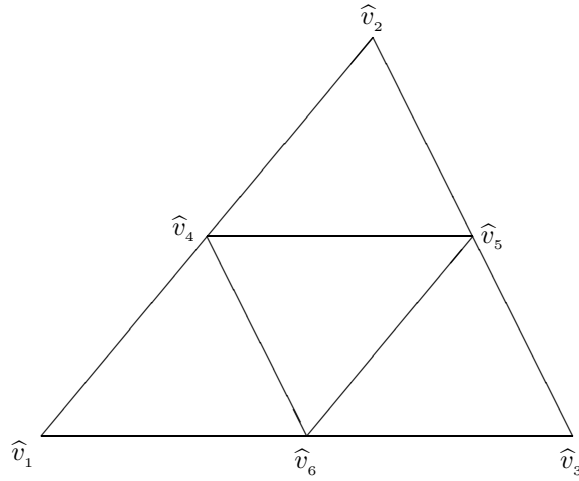


FIGURE 1. Symmetric triangulation.

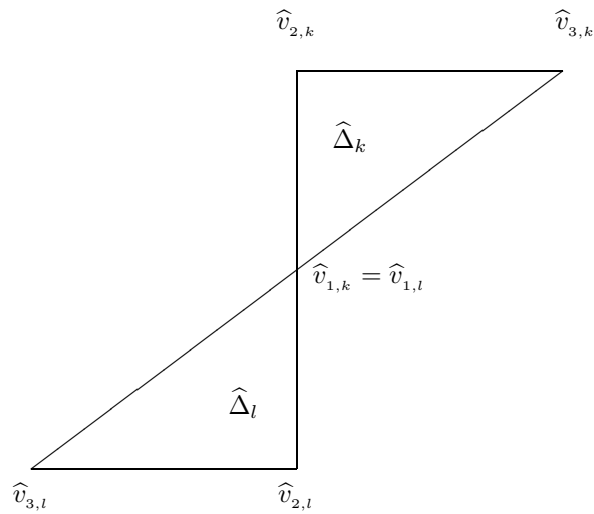


FIGURE 2. A symmetric pair of triangles.

We will refer to triangulations with this form of refinement as *symmetric triangulations*. The property of symmetry will increase the degree of precision of a quadrature formula which we will use in this paper. An-

other important feature is that the set of all vertices of triangles in the triangulation τ_n is a subset of all vertices of τ_{n+1} . This will reduce the number of function evaluations when approximating a definite integral, eventually leading to a fast algorithm of numerical integration.

With this special type of refinement strategy for the triangulation, the collocation method with piecewise quadratic approximations has superconvergence results for a collocation solution [8]. In most practical problems, the evaluation of the integrals for the matrix elements in the collocation system will require numerical integration. And the calculation of some matrix elements needs special attention when the kernel is weakly singular or nearly weakly singular. A numerical integration scheme for collocation integrals is given in Section 5. It is based on another type of special refinement which is called an ‘ $La + u$ ’ refinement about P with L a positive integer and P a vertex of a triangle Δ . The remainder of this section is devoted to the presentation of the ‘ $La + u$ ’ refinement. The superconvergence of the approximate solution associated with the numerical integration scheme is proven in Section 5.

For simplicity, we assume Δ is a planar triangle. The initial triangulation τ_1 of Δ is obtained by connecting the midpoints of the sides of Δ using straight lines. Then τ_1 consists of four new triangles. To obtain τ_2 , we divide the triangle containing the vertex P into four new triangular elements. For the resulting triangulation, repeat the preceding subdivision. After doing this L times, we divide simultaneously every triangle into four new triangles. The final triangulation produces $\tau_2 = \{\Delta_{k,2} \mid k = 1, \dots, N_2\}$. In general to get from level n to level $n+1$, we perform L times an adaptive subdivision on a triangle containing P , and then we do one simultaneous subdivision of all triangles. Thus, the mesh size $\delta_n \rightarrow 0$ as $n \rightarrow \infty$. An advantage of this form of refinement is that each set of mesh points contains those at the preceding level.

As an example, we illustrate the ‘ $2a + u$ ’ refinement for $n = 1, 2$ in Figures 3 and 4. When $n = 2$, there are three regions in Δ , each of which is divided by symmetric triangulation, but with different levels of subdivision. So the triangles in τ_2 vary in size. Note that there are only three different triangular elements in size. A finer mesh is placed near the vertex, where the integrand usually is ill-behaved, to improve the performance of a standard quadrature method.

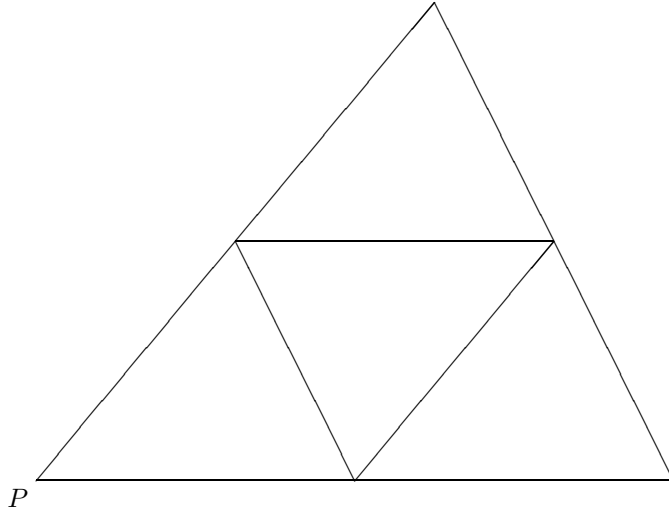


FIGURE 3. $n = 1$.

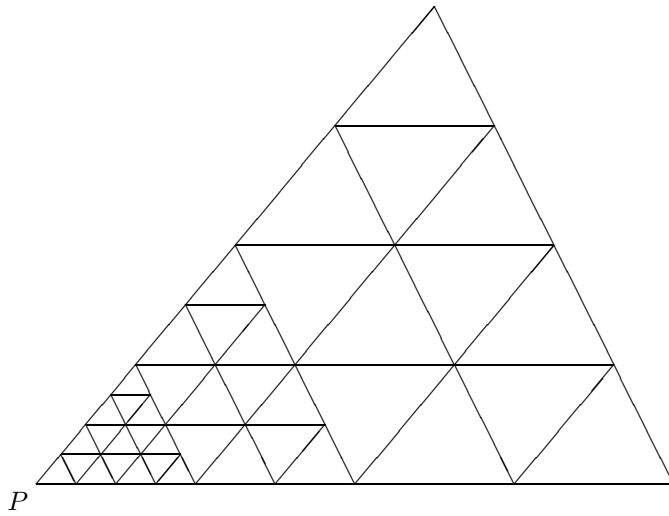


FIGURE 4. $n = 2$.

More generally, by examining the structure of the ‘ $La+u$ ’ refinement, we can calculate the total number N_n of triangles at level n : this is $(L+1)2^{2n} - 4L = O(2^{2n})$. There are $Ln - (L-1)$ different triangular elements in size. The closer the triangle is to the point P , the smaller it is. As the triangles vary in size from large to small, we name the region containing the triangles of the same size to be $B_0, B_1, \dots, B_{Ln-L}$, respectively. The diameter of triangles in B_l , denoted by r_l , is $O(2^{-(n+l)})$. Then the mesh size is

$$\delta_n = \max_{0 \leq l \leq Ln-L} r_l = r_0 = O(2^{-n})$$

and

$$(2.6) \quad O(\delta_n) = O(N_n^{-1/2}).$$

Let N_l be the number of triangles in B_l . Then N_l is proportional to 4^{n-i} where $l = iL + i_1$ for $0 \leq i_1 \leq L-1$. The distance from the point P to B_l , denoted by d_l , is $O(1/2^{(L+1)(l-i_1)/L})$.

If $L=0$, then the ‘ $La+u$ ’ refinement is the symmetric triangulation. The analysis given in [9] indicates that the symmetric triangulation is a better scheme to use with smooth integrands in the numerical integration, while a graded mesh is needed with the singular integrals. See [28].

3. Interpolation. Let σ denote the unit simplex in the st -plane

$$\sigma = \{(s, t) \mid 0 \leq s, t, s+t \leq 1\}.$$

Let ρ_1, \dots, ρ_6 denote the three vertices and three midpoints of the sides of σ , numbered according to Figure 5.

To define interpolation, introduce the basis functions for quadratic interpolation on σ . Letting $u = 1 - (s+t)$, define

$$\begin{aligned} l_1(s, t) &= u(2u-1), & l_2(s, t) &= t(2t-1), & l_3(s, t) &= s(2s-1), \\ l_4(s, t) &= 4tu, & l_5(s, t) &= 4st, & l_6(s, t) &= 4su. \end{aligned}$$

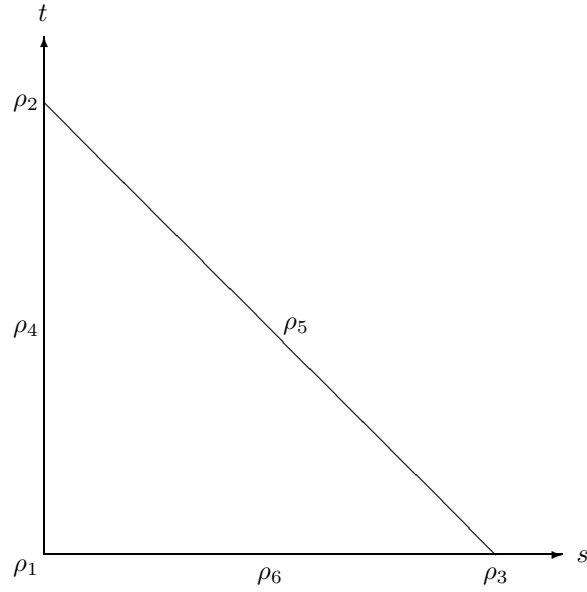


FIGURE 5. The unit simplex.

We give the corresponding set of basis functions $\{l_{j,k}(q)\}$ on Δ_k by using its parametrization over σ . Let $\hat{\Delta}_k$ be an element in the triangulation of R_j , corresponding to Δ_K , and let \hat{v}_1, \hat{v}_2 and \hat{v}_3 be its vertices. Define

$$(3.1) \quad m_k(s, t) = F_j(u\hat{v}_1 + t\hat{v}_2 + s\hat{v}_3), \quad u = 1 - s - t, \quad (s, t) \in \sigma,$$

where $F_j : R_j \xrightarrow{1-1}_{\text{onto}} S_j$ is a five-times continuously differentiable function. Then m_k is a bijective mapping from σ to Δ_k with $m_k \in C^5(\sigma)$. Introduce the node points for Δ_k by $v_{j,k} = m_k(\rho_j)$, $j = 1, \dots, 6$. The first three are the vertices and the last three are approximate midpoints of the sides of Δ_k . Define

$$l_{j,k}(m_k(s, t)) = l_j(s, t), \quad j = 1, \dots, 6, \quad k = 1, \dots, N.$$

Given a function f , define

$$(3.2) \quad \mathcal{P}_N f(q) = \sum_{j=1}^6 f(v_{j,k}) l_{j,k}(q), \quad q \in \Delta_k,$$

for $k = 1, \dots, N$. This is called the *piecewise quadratic function interpolating f* on the nodes of the mesh $\{\Delta_k \mid k = 1, \dots, N\}$ for S . Although our analysis is using quadratic approximation, the method can be generalized to using other degrees of piecewise polynomial approximation. The error analysis is the same except that the argument is somewhat more complicated.

It is straightforward that \mathcal{P}_N is a bounded projection operator and $\|\mathcal{P}_N\| = 5/3$. Also, for any $f \in C^3(S)$,

$$(3.3) \quad \|f - \mathcal{P}_N f\|_\infty = O(\hat{\delta}_N^3)$$

where $\hat{\delta}_N$ is the mesh size of the triangulation $\{\hat{\Delta}_k \mid k = 1, \dots, N\}$ of R_j 's. See [2].

The numerical integration formula used in this paper is

$$(3.4) \quad \int_\sigma g(s, t) ds dt \approx \frac{1}{6} [g(\rho_4) + g(\rho_5) + g(\rho_6)]$$

which is based on integrating the quadratic polynomial interpolating g on σ at ρ_1, \dots, ρ_6 . This integration has degree of precision two, integrating exactly all quadratic polynomials.

With the triangulation $\{\Delta_k\}$ and the mappings $m_k : \sigma \xrightarrow{1-1} \Delta_k$, we have

$$(3.5) \quad \int_{\Delta_k} f(q) dS = \int_\sigma f(m_k(s, t)) |D_s m_k(s, t) \times D_t m_k(s, t)| ds dt.$$

D_s and D_t denote differentiation with respect to s and t , respectively. The quantity $|D_s m_k(s, t) \times D_t m_k(s, t)|$ is the Jacobian determinant of the mapping $m_k(s, t)$ used in transforming surface integrals over Δ_k into integrals over σ . When Δ_k is a planar triangle, the Jacobian is twice the area of Δ_k .

Applying (3.4) to the right side of (3.5), we have

$$(3.6) \quad \int_{\Delta_k} f(q) dS \approx \frac{1}{6} \sum_{j=4}^6 f(m_k(\rho_j)) |D_s m_k(s, t) \times D_t m_k(s, t)|_{\rho_j}.$$

A major problem with (3.6) is that $D_s m_k$ and $D_t m_k$ are inconvenient to compute for some elements Δ_k on many surfaces S . Therefore, we

use interpolation to approximate $m_k(s, t)$ in terms of only its values at ρ_1, \dots, ρ_6 . Define

$$\tilde{m}_k(s, t) = \sum_{j=1}^6 m_k(\rho_j) l_j(s, t) = \sum_{j=1}^6 v_{j,k} l_j(s, t).$$

Thus, $\tilde{m}_k(s, t)$ interpolates $m_k(s, t)$ at ρ_1, \dots, ρ_6 , and each component is quadratic in (s, t) . Then

$$(3.7) \quad \begin{aligned} \int_{\Delta_k} f(q) dS &\approx \frac{1}{6} \sum_{j=4}^6 f(m_k(\rho_j)) |D_s \tilde{m}_k(s, t) \times D_t \tilde{m}_k(s, t)|_{\rho_j} \\ &= \sum_{j=4}^6 \tilde{\omega}_{j,k} f(v_{j,k}) \end{aligned}$$

where

$$\tilde{\omega}_{j,k} = |D_s \tilde{m}_k(s, t) \times D_t \tilde{m}_k(s, t)|_{\rho_j} / 6.$$

4. The collocation method. Any collocation method for solving an integral equation $(\lambda + \mathcal{K})\rho = g$ can be written as

$$(4.1) \quad (\lambda + \mathcal{P}_N \mathcal{K})\rho_n = \mathcal{P}_N g, \quad \lambda = 2\pi.$$

The function g can be the function f of (1.3) or $\mathcal{S}f$ of (1.6). For our work, the operator \mathcal{P}_N is the projection operator defined by (3.2). We discuss results for this approximation; and then in the next section, we give error results for the discrete collocation method which is based on the numerical integration scheme given in [27] and [28].

For S being smooth, the solvability of (4.1) is determined from the standard theory for projection methods; for example, see Atkinson [1, p. 50–62]. With the assumption of (a) compactness for $\mathcal{K} : C(S) \rightarrow C(S)$ and (b) pointwise convergence on $C(S)$ of the projections \mathcal{P}_N to I , we have that

$$\|(I - \mathcal{P}_N)\mathcal{K}\|_{\infty} \rightarrow 0 \quad \text{as } n \rightarrow \infty.$$

From this, we have the standard result that if $(\lambda + \mathcal{K})^{-1}$ exists on $C(S)$, then $(\lambda + \mathcal{P}_N \mathcal{K})^{-1}$ exists and is uniformly bounded for all sufficiently large N , say $N \geq N_0$.

In [8], Atkinson and Chien considered the iterated collocation solution

$$\hat{\rho}_n = \frac{1}{\lambda}(g - \mathcal{K}\rho_n).$$

It satisfies the equations

$$(4.2) \quad (\lambda + \mathcal{K}\mathcal{P}_N)\hat{\rho}_n = g$$

$$(4.3) \quad \mathcal{P}_N\hat{\rho}_n = \rho_n.$$

The questions of stability for (4.1) and (4.2) are linked by the identities

$$(4.4) \quad \begin{aligned} (\lambda + \mathcal{K}\mathcal{P}_N)^{-1} &= \frac{1}{\lambda}[I - \mathcal{K}(\lambda + \mathcal{P}_N\mathcal{K})^{-1}\mathcal{P}_N] \\ (\lambda + \mathcal{P}_N\mathcal{K})^{-1} &= \frac{1}{\lambda}[I - \mathcal{P}_N(\lambda + \mathcal{K}\mathcal{P}_N)^{-1}\mathcal{K}]. \end{aligned}$$

The existence of uniform boundedness of $(\lambda + \mathcal{K}\mathcal{P}_N)^{-1}$ then follows from (4.4).

The errors in ρ_n and $\hat{\rho}_n$ can be expressed as

$$\begin{aligned} \rho - \rho_n &= \lambda(\lambda + \mathcal{P}_N\mathcal{K})^{-1}(\rho - \mathcal{P}_N\rho) \\ \rho - \hat{\rho}_n &= -(\lambda + \mathcal{K}\mathcal{P}_N)^{-1}\mathcal{K}(\rho - \mathcal{P}_N\rho). \end{aligned}$$

The quantity $\mathcal{K}(\rho - \mathcal{P}_N\rho)$ sometimes converges to zero more rapidly than does $\rho - \mathcal{P}_N\rho$. Using (4.3), it can be shown that ρ_n is superconvergent to ρ at the collocation node points, and we will make use of this in the following.

Theorem 1. *Consider the integral equation (1.3) and (1.6) with solution ρ . Let S be a smooth surface in \mathbf{R}^3 , and assume the unknown function $\rho \in C^4(S)$. Then*

$$(4.5) \quad \max_{1 \leq i \leq N_v} |\rho(v_i) - \rho_n(v_i)| = O(\hat{\delta}_n^4 \ln \hat{\delta}_n)$$

where $\hat{\delta}_n$ is the mesh size of the triangulation $\{\hat{\Delta}_{k,n} | k = 1, \dots, N_n\}$ of the R_j 's obtained by the symmetric triangulation. The set $\{v_i | i = 1, \dots, N_v\}$ is the collection of the node points of the triangulation $\{\Delta_{k,n}\}$ with N_v the number of distinct node points.

Proof. See [8]. \square

5. A discrete collocation method. Given $\{v_i \mid i = 1, \dots, N_v\}$, the collection of the node points of the triangulation, the linear system for (4.2) becomes

$$(5.1) \quad 2\pi\hat{\rho}_n(v_i) + \sum_{k=1}^{N_n} \sum_{j=1}^6 \hat{\rho}_n(v_{j,k}) \int_{\sigma} \kappa(v_i, m_k(s, t)) l_j(s, t) \cdot |D_s m_k \times D_t m_k| d\sigma = g(v_i), \quad i = 1, \dots, N_v$$

where $\kappa(P, Q)$ denotes the kernel function for the double layer integral operator, i.e.,

$$\kappa(P, Q) = \frac{\partial}{\partial \nu_Q} \left[\frac{1}{|P - Q|} \right].$$

Let $2\pi I + K_N$ be the matrix of coefficients of (5.1). Then we can write (5.1) as

$$(5.2) \quad (2\pi I + K_N)\hat{\rho}_n = g_n$$

where $\hat{\rho}_n = (\hat{\rho}_n(v_i))$, $g_n = (g(v_i))$. By the equation (4.3), $\hat{\rho}_n(v_i) = \rho_n(v_i)$ for $i = 1, \dots, N_v$; and then (5.2) becomes

$$(2\pi I + K_N)\rho_n = g_n$$

where $\rho_n = (\rho_n(v_i))$.

The collocation integrals in the matrix of coefficients K_N are given by

$$(5.3) \quad \int_{\sigma} \kappa(v_i, m_k(s, t)) l_j(s, t) |D_s m_k \times D_t m_k| d\sigma$$

and (5.3) must be evaluated numerically for $i = 1, \dots, N_v$, $j = 1, \dots, 6$ and $k = 1, \dots, N_n$. For the exterior Neumann problem, we also need to evaluate numerically the corresponding single layer integrals

$$(5.4) \quad \int_{\sigma} \frac{f(m_k(s, t))}{|v_i - m_k(s, t)|} |D_s m_k \times D_t m_k| ds.$$

We consider two cases in evaluating (5.3), depending on whether v_i is inside or outside of $\Delta_{k,n}$. The numerical integration method being used is (3.4). We also use the approximate surface \tilde{m}_k . The following scheme is based on the error analyses in [27, 28].

Case 1. If $v_i \in \Delta_{k,n}$, then $\kappa(v_i, Q)$ is singular at $Q = v_i$. The singularity of the integrand in (5.3) is $1/|v_i - Q|$ as $Q \rightarrow v_i$ (see [27]). The interpolation-based numerical integration associated with the ‘ $La+u$ ’ refinement for this type of function has been studied in [28]. It was shown that to retain the optimal rate of convergence $O(1/N^2)$, or $O(\delta_n^4)$ by (2.6), as for smooth integrands, the value of L must be greater than 3. Here N means the total number of triangles in the triangulation of a triangular element at level n , δ_n the mesh size of the triangulation. It motivates us to use the ‘ $4a+u$ ’ refinement to further divide the element $\Delta_{k,n}$ for the purpose of numerically evaluating (5.3) and (5.4). Assume the collocation node v_i is a vertex, say $v_i = m_k(0, 0)$. We perform n loops of ‘ $4a+u$ ’ refinement about $(0, 0)$ on σ , and then we integrate (5.3) by applying (3.7) to each of the integrals over each of the corresponding subtriangles. If the collocation node v_i is a midpoint of a side, then we split $\Delta_{k,n}$ into two parts (see Figure 6) and treat the integral over each part as described above.

Case 2. For $v_i \notin \Delta_{k,n}$, the integrand in (5.3) is analytic; but it is increasingly peaked as the distance between v_i and $\Delta_{k,n}$ decreases. We numerically evaluate these integrals in the following way.

If

$$0 < \text{dist}(v_i, \Delta_{k,n}) \leq (2-1)\delta_n,$$

where δ_n is the mesh size of $\{\Delta_{k,n}\}$ as defined in (2.5), then integrate (5.3) using (3.7) with n levels of symmetric triangulation of $\Delta_{k,n}$ (thus dividing $\Delta_{k,n}$ into 4^n congruent subtriangles, with (3.7) applied to the integral over each of the corresponding subtriangles). If $v_i \notin \Delta_{k,n}$ and

$$(2-1)\delta_n < \text{dist}(v_i, \Delta_{k,n}) \leq (2^2-1)\delta_n,$$

then integrate (5.3) using (3.7) with $\max\{n-1, 1\}$ levels of symmetric triangulation of $\Delta_{k,n}$. If $v_i \notin \Delta_{k,n}$ and

$$(2^2-1)\delta_n < \text{dist}(v_i, \Delta_{k,n}) \leq (2^3-1)\delta_n,$$

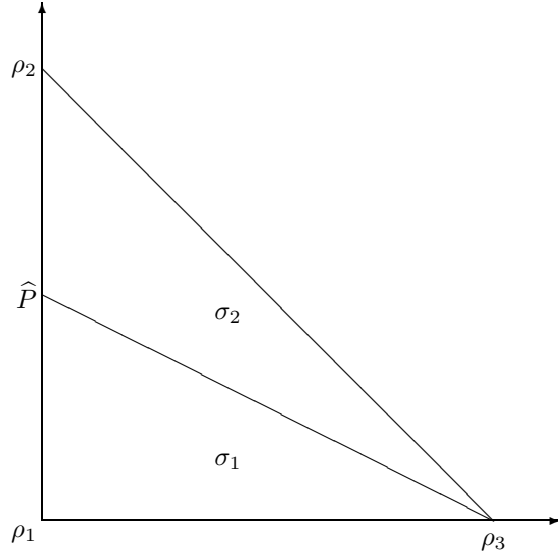


FIGURE 6. Splitting triangles.

then integrate (5.3) using (3.7) with $\max\{n-2, 1\}$ levels of symmetric triangulation of $\Delta_{k,n}$. Continue with this in the obvious way. A similar method of numerical integration for $v_i \notin \Delta_{k,n}$ was suggested in [8], without analysis.

Analysis of quadrature error. Consider the error from evaluating (5.3) over S associated with the resulting triangulation. We have found that the error is $O(\hat{\delta}_n^4)$, where $\hat{\delta}_n$ is the mesh size of $\hat{\Delta}_{k,n}$. The argument is more complicated than the one used in [27], because there are many more triangles within a small distance of the point v_i .

The integrand in (5.3) varies from singular to quite smooth. To handle this varied behavior, we classify triangles in the triangulation $\{\Delta_{k,n}\}$ into two groups. Let T_1 be the collection of triangles $\Delta_{k,n}$ containing P , let T_2 be the collection of triangles $\Delta_{k,n}$ with $P \notin \Delta_{k,n}$. Let E_i denote the error contributed by T_i for $i = 1, 2$.

Case 1. According to the numerical integration scheme, each triangle $\Delta_{k,n} \in T_1$ is further divided by the ‘ $4a + u$ ’ refinement. Let $\hat{\delta}_{k,n}^*$ be the mesh size of the resulting triangulation for $\hat{\Delta}_{k,n}$, then the error contributed by each triangle $\Delta_{k,n}$ is $O(\hat{\delta}_{k,n}^{*4})$ by Lemma 1 in [27]. Since the number of triangles $\Delta_{k,n}$ in T_1 is finite, in fact, at most 6, therefore $E_1 = O(\hat{\delta}_{k,n}^{*4})$. Notice that $\hat{\delta}_{k,n}^* = O((1/2^n)\hat{\delta}_n)$, the error E_1 is much smaller than $O(\hat{\delta}_n^4)$.

Case 2. For the error from T_2 , the collection of triangles not containing v_i , we note that the size of triangles in T_2 varies. The quadrature mesh size becomes larger as the distance from v_i increases. We examine the structure of T_2 based on the triangulation of a generic $\Delta_{k,n}$. Define

$$\begin{aligned} d_{k,n} &= \text{dist}(v_i, \Delta_{k,n}) \\ d_n &= \min_k \{d_{k,n} \mid d_{k,n} > 0\} \\ \hat{\delta}_n &= \text{the mesh size of } \{\hat{\Delta}_{k,n}\}. \end{aligned}$$

Then $d_n = O(\hat{\delta}_n)$ and $\hat{\delta}_n = O(\hat{\delta}/2^n)$, with $\hat{\delta}$ the mesh size of the original parametrization domains $\{R_j \mid j = 1, \dots, J\}$. To simplify the argument, without any loss of generality, we take $d_{k,n} \doteq d_n, 2d_n, \dots$, depending on how far the $\Delta_{k,n}$ is from the point v_i . And the number of $\Delta_{k,n}$ at distance $i \cdot d_n$ is proportional to i . Define

$$A_m^{(n)} = \{\Delta_{k,n} \mid (2^m - 1) \cdot d_n \leq d_{k,n} < (2^{m+1} - 1) \cdot d_n\}$$

for $m = 1, 2, \dots, m(n)$. The value of $m(n)$ is at most n because we only consider triangles near the node point v_i . With the refinement we used, we know that each triangle in $A_m^{(n)}$ is divided into 4^{n-m} subtriangles uniformly. There are two types of triangles in $A_m^{(n)}$. Those triangles that are part of symmetric pairs of triangles (cf. Figure 2) are of the first type and remaining triangles are of the second type. Denote triangles in $A_m^{(n)}$ by $\Delta_{k,n}^*$.

Define

$$A_{mj}^{(n)} = \left\{ \Delta_{k,n}^* \subset A_m^{(n)} \mid (2^m - 1) \cdot d_n + j \frac{\hat{\delta}_n}{2^{n-m}} \leq \text{dist}(v_i, \Delta_{k,n}^*) < (2^m - 1) \cdot d_n + (j+1) \frac{\hat{\delta}_n}{2^{n-m}} \right\},$$

$$j = 0, 1, \dots, t_m - 1$$

where $t_m \leq O(2^n)$ because $d_n = O(\hat{\delta}_n)$. Let c_{mj} , c'_{mj} be the numbers of triangles of the first type and the second type at distance $(2^m - 1) \cdot d_n + j(\hat{\delta}_n/2^{n-m})$, respectively. Then $c_{mj} = O(2^m 2^{n-m}) = O(2^n)$, $c'_{mj} = O(1)$. In addition, $\hat{\delta}_{k,n}^*$, the mesh size of $A_{mj}^{(n)}$ is $\hat{\delta}_n/2^{n-m}$. Let $d_{k,n}^* \equiv \text{dist}(v_i, \Delta_{k,n}^*)$, $d_{k,n}^* \geq (2^m - 1) \cdot d_n + j\hat{\delta}_n/2^{n-m}$ for triangles $\Delta_{k,n}^* \subset A_{mj}^{(n)}$.

Following an argument similar to that in [27], the error from the numerical integration over triangles of the first type in $A_m^{(n)}$ is bounded by

$$\begin{aligned} \sum_{j=0}^{t_m-1} c_{mj} O\left(\frac{\hat{\delta}_{k,n}^*{}^6}{d_{k,n}^*{}^5}\right) &= \sum_{j=0}^{t_m-1} O(2^n) O\left(\frac{\hat{\delta}_{k,n}^*{}^6}{d_{k,n}^*{}^5}\right) \\ &\leq \sum_{j=0}^{t_m-1} O(2^n) O\left(\left[\frac{\hat{\delta}_n}{2^{n-m}}\right]^6 \frac{1}{[(2^m-1) \cdot d_n + j\hat{\delta}_n/(2^{n-m})]^5}\right) \\ &\leq \sum_{j=0}^{t_m-1} O(2^n) O\left(\frac{\hat{\delta}_n^6}{2^{6n-6m}} \frac{1}{(2^m-1)^5 \cdot d_n^5}\right) \\ &\leq \sum_{j=0}^{t_m-1} O(2^n) O\left(\hat{\delta}_n \frac{1}{2^{6n-6m}} \frac{1}{2^{5m}}\right) \\ &\leq O(2^n) O(2^n) O\left(\frac{1}{2^n} \frac{1}{2^{6n-6m}} \frac{1}{2^{5m}}\right) \\ &= O\left(\frac{1}{2^{4n}} \frac{1}{2^{n-m}}\right). \end{aligned}$$

The error from the numerical integration over triangles of the second

type in $A_m^{(n)}$ is bounded by

$$\begin{aligned}
\sum_{j=0}^{t_m-1} c'_{mj} O\left(\frac{\hat{\delta}_{k,n}^* 5}{d_{k,n}^* 4}\right) &= \sum_{j=0}^{t_m-1} O(1) O\left(\frac{\hat{\delta}_{k,n}^* 5}{d_{k,n}^* 4}\right) \\
&\leq \sum_{j=0}^{t_m-1} O\left(\left[\frac{\hat{\delta}_n}{2^{n-m}}\right]^5 \frac{1}{[(2^m-1) \cdot d_n + j\hat{\delta}_n/(2^{n-m})]^4}\right) \\
&\leq \sum_{j=0}^{t_m-1} O\left(\hat{\delta}_n \frac{1}{2^{5n-5m}} \frac{1}{2^{4m}}\right) \\
&\leq O(2^n) O\left(\frac{1}{2^n} \frac{1}{2^{5n-m}}\right) \\
&= O\left(\frac{1}{2^{4n}} \frac{1}{2^{n-m}}\right).
\end{aligned}$$

Consequently, the error from $A_m^{(n)}$ is $O((1/2^{4n})(1/2^{n-m}))$.

The error from the numerical integration over T_2 is bounded by

$$\sum_{m=1}^{m(n)} O\left(\frac{1}{2^{4n}} \frac{1}{2^{n-m}}\right) = O\left(\frac{1}{2^{4n}}\right) = O(\hat{\delta}_n^4).$$

By a similar calculation, we can show that the error from the approximate surface \tilde{m} over T_2 is also $O(1/2^{4n}) = O(\hat{\delta}_n^4)$. Hence, $E_2 = O(\hat{\delta}_n^4)$.

Combining the above error analysis and noticing that the error from the single layer integral (5.4) can be obtained in the same way, we give the global error for the single layer and double layer integrals in the following theorem.

Theorem 2. *Let S , $\{\Delta_{k,n}\}$, $\{v_i\}$, $\hat{\delta}_n$ be as in Theorem 1. Assume that $f \in C^4(S)$. Let $\tilde{\mathcal{S}}_n(f), \tilde{\mathcal{D}}_n(f)$ be the numerical integration associated with the scheme given above for the single layer integral and double layer integral, respectively. Then*

$$(5.5) \quad \max_{1 \leq i \leq N_v} \left| \int_S \frac{f(Q)}{|v_i - Q|} dS_Q - \tilde{\mathcal{S}}_n(f) \right| = O(\hat{\delta}_n^4)$$

$$(5.6) \quad \max_{1 \leq i \leq N_v} \left| \int_S f(Q) \frac{\partial}{\partial \nu_Q} \left[\frac{1}{|v_i - Q|} \right] dS_Q - \tilde{\mathcal{D}}_n(f) \right| = O(\hat{\delta}_n^4).$$

The method being used has retained the same rate of convergence as the one with uniform meshes for smooth integrands. Nonetheless, the integration of (5.3) and (5.4) are still the most expensive parts of our computation. Several methods have been tried for evaluating (5.3) and (5.4). Besides the method suggested in Atkinson and Chien [8], a method with automatic error control could be based on what was described in Atkinson [3] and [5]. Numerical quadratures with no approximation of the surface was presented in Guermond and Fontaine [14] and Guermond [13]. But we believe our method is easier to implement and gives a better approximation.

With the preceding numerical integration scheme, the collocation integrals in K_N are evaluated numerically. The resulting linear system is denoted by

$$(5.7) \quad (2\pi I + \tilde{K}_N)\tilde{\rho}_n = \tilde{g}_n$$

where

$$\begin{aligned} \tilde{\rho}_n &= (\tilde{\rho}(v_1), \tilde{\rho}(v_2), \dots, \tilde{\rho}(v_{N_v})) \\ \tilde{g}_n &= (\tilde{g}(v_1), \tilde{g}(v_2), \dots, \tilde{g}(v_{N_v})) \\ \tilde{g}(v_i) &\equiv \begin{cases} f(v_i) & \text{if } g = f \\ \tilde{\mathcal{S}}_n(f)(v_i) & \text{if } g = \mathcal{S}f. \end{cases} \end{aligned}$$

Recall that $\tilde{\mathcal{S}}_n(f)(v_i)$ is the preceding numerical integration for the single layer integral at $P = v_i$. The vector $\tilde{\rho}_n$ is called the *discrete collocation solution*, and it is more explicitly computable than ρ_n or $\hat{\rho}_n$.

The error analyses of layer potentials help us establish the rate of convergence of the discrete collocation method.

Theorem 3. *Consider the integral equations (1.3) and (1.6) with solution ρ . Let S be a smooth surface in \mathbf{R}^3 , and assume the unknown function $\rho \in C^4(S)$. Then*

$$(5.8) \quad \max_{1 \leq i \leq N_v} |\rho(v_i) - \tilde{\rho}_n(v_i)| = O(\hat{\delta}_n^4 \ln \hat{\delta}_n).$$

Proof. We use a perturbation analysis, based on regarding the system (5.7) as a perturbation of the corresponding linear system (5.2)

$$(2\pi I + K_N)\rho_n = g_n.$$

As noted earlier following (4.4), $(2\pi + \mathcal{K}\mathcal{P}_N)^{-1}$ is uniformly bounded for all sufficiently large N . Also, since the iterated collocation equation can be considered as being a Nyström method, we have that $(2\pi I + K_N)^{-1}$ exists (see Atkinson [1, p. 88–93]). Moreover, we can bound $\|(2\pi I + K_N)^{-1}\|_\infty$ in terms of c by following a standard derivation, where the matrix norm $\|\cdot\|_\infty$ is the standard matrix row norm.

For any $G \in \mathbf{R}^{N_v}$ with N_v the number of node points, we choose a function $g \in C(S)$ with

$$g(v_j) = G_j, \quad j = 1, \dots, N_v$$

and

$$\|g\|_\infty = \|G\|_\infty.$$

Then the solution of the approximating equation

$$(2\pi + \mathcal{K}\mathcal{P}_N)\rho_n = g$$

in $C(S)$, and the solution of the linear system

$$(2\pi I + K_N)Z = G$$

in \mathbf{R}^{N_v} are related by $\rho_n(v_j) = Z_j$, $j = 1, \dots, N_v$. Therefore,

$$\begin{aligned} \|(2\pi I + K_N)^{-1}G\|_\infty &= \|Z\|_\infty \leq \|\rho_n\|_\infty \\ &= \|(2\pi + \mathcal{K}\mathcal{P}_N)^{-1}g\|_\infty \\ &\leq \|(2\pi + \mathcal{K}\mathcal{P}_N)^{-1}\|_\infty \|g\|_\infty \\ &= \|(2\pi + \mathcal{K}\mathcal{P}_N)^{-1}\|_\infty \|G\|_\infty. \end{aligned}$$

This implies that

$$(5.9) \quad \begin{aligned} \|(2\pi I + K_N)^{-1}\|_\infty &\leq \|(2\pi + \mathcal{K}\mathcal{P}_N)^{-1}\|_\infty \\ &\leq c < \infty, \quad N \geq N_0. \end{aligned}$$

The present analysis uses the result

$$(5.10) \quad \|K_N - \tilde{K}_N\|_\infty = O\left(\frac{1}{2^{4n}}\right) = O(\delta_n^4)$$

with the matrix row norm. The proof of (5.10) is essentially the same as the one for (5.6). Using (5.10) and the invertibility of $2\pi I + K_N$ with the uniform boundedness of $(2\pi I + K_N)^{-1}$ for all sufficiently large N , the geometric series theorem implies that

$$[I - (2\pi I + K_N)^{-1}(K_N - \tilde{K}_N)]^{-1}$$

exists and is bounded by

$$(5.11) \quad \frac{1}{1 - \|(2\pi I + K_N)^{-1}(K_N - \tilde{K}_N)\|_\infty}.$$

Therefore,

$$2\pi I + \tilde{K}_N = (2\pi I + K_N)[I - (2\pi I + K_N)^{-1}(K_N - \tilde{K}_N)]$$

is invertible and the inverse of $2\pi I + \tilde{K}_N$ is uniformly bounded for some sufficiently large N_0 .

By straightforward manipulation of (5.7) and (5.2), we have

$$(5.12) \quad \begin{aligned} \rho_n - \tilde{\rho}_n &= (2\pi I + \tilde{K}_N)^{-1}[\tilde{K}_N - K_N]g_n \\ &\quad + (2\pi I + \tilde{K}_N)^{-1}[g_n - \tilde{g}_n]. \end{aligned}$$

The first term on the right side is $O(\delta_n^4)$, from (5.10). The second term is either zero or $O(\delta_n^4)$, from (5.5). When considered with Theorem 1, this shows the result (5.8). \square

Comparing Theorem 3 with the result stated in Theorem 1, the error formula (5.8) is for the computable approximate solution $\tilde{\rho}_n$. The same error estimate in (4.5) is for the collocation solution ρ_n with exact integration over the true surface, which is originally proven in [8]. The error analysis shows that our numerical integration scheme has given sufficiently accurate approximations of collocation integrals to match the accuracy of the collocation solution ρ_n .

6. Numerical examples. The integral equations (1.3) and (1.6) are different only in their right-hand inhomogeneous term. With (1.6), we can study the error in the numerical solution of the integral

equation by using problems for which we know the true solution of (1.4). With equation (1.3), we do not know the true solution in general (except when $f \equiv 1$); and thus the numerical solution must be checked indirectly by evaluating (1.2) numerically and comparing it to a known solution u . Our numerical examples are given for the exterior Neumann problem only.

Two smooth surfaces were used in our experiments. Surface #1 (denoted by S#1) was the ellipsoid

$$\left(\frac{x}{a}\right)^2 + \left(\frac{y}{a}\right)^2 + \left(\frac{z}{c}\right)^2 = 1$$

with $a, b, c > 0$.

The ellipsoid is convex and symmetric. For that reason, we also devised and used a surface which is not symmetric and which is slightly nonconvex. Surface #2 (S#2) is defined by

$$(x, y, z) = \rho(\xi, \eta, \zeta)(A\xi, B\eta, C\zeta), \quad \xi^2 + \eta^2 + \zeta^2 = 1$$

with

$$\rho(\xi, \eta, \zeta) = 1 - [(\xi - .1)^2 + 2(\eta - .1)^2 - 3(\zeta - .1)^2]/\alpha$$

and $A, B, C > 0$, $\alpha \geq 2.43$. The case we use here is $\alpha = 10$ and $(A, B, C) = (2, 2, 1)$. Figure 7 gives the cross-sections of S#2 when intersecting S with vertical planes containing the z -axis, intersecting at angles of $\phi = 0, \pi/4, \pi/2$ with respect to the positive x -axis.

We begin with the solution of (1.4) for the ellipsoid (S#1)

$$\left(\frac{x}{a}\right)^2 + \left(\frac{y}{b}\right)^2 + \left(\frac{z}{c}\right)^2 = 1$$

with $(a, b, c) = (2, 2.5, 3)$. The exterior Neumann problem (1.4) was solved with the function f so chosen that the true solution is known. The two cases used here are

$$(6.1) \quad u_1(P) = \frac{1}{r}, \quad u_2(P) = \frac{1}{r} e^{x/r^2} \cos(z/r^2)$$

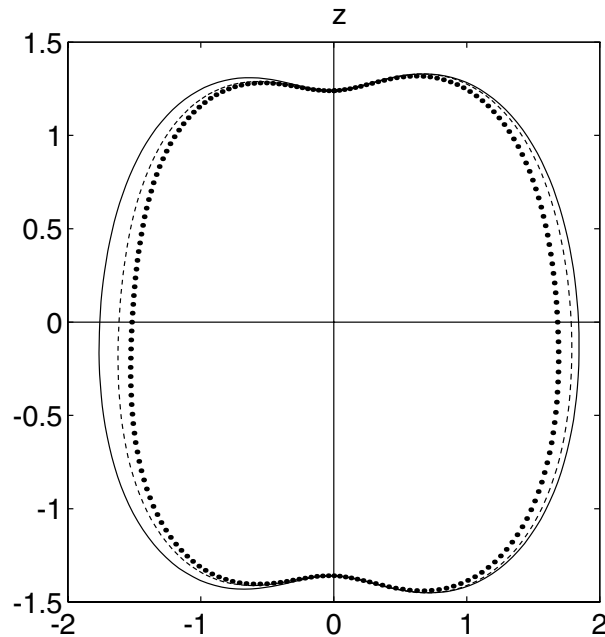


FIGURE 7. Cross sections of “squash” surface. Solid curve: $\phi = 0$; dash curve: $\phi = \pi/4$; dot curve: $\phi = \pi/2$.

with $P = (x, y, z)$ and $r = |P|$. In this case $\rho = u_m$, and we use u_m and $u_{m,n}$, $m = 1, 2$, for the true solution and the discrete collocation solution at level n in our discussion, respectively. We initially divide the surface into eight triangular elements. Each of these elements is a portion of the surface within one octant.

The method was implemented with a package of programs written by K. Atkinson, which is described in [2, 7]. All examples were computed on a Hewlett-Packard workstation in double precision arithmetic. Table 1 contains the maximum error at the node points for solving boundary integral equation (1.6). The column labeled *Ratio* gives the value E_n/E_{n+1} where $E = \|u_m - u_{m,n}\|_\infty$ is the error at level n . The results are consistent with an asymptotic rate for the error of $O(\hat{\delta}_n^4)$ or $O(\hat{\delta}_n^4 \ln \hat{\delta}_n)$, in agreement with the theoretical result in Theorem 3. Here n , N_n and $\hat{\delta}_n$ are defined as before.

TABLE 1. Maximum errors on ellipsoid S#1.

n	N_n	$\ u_1 - u_{1,n}\ _\infty$	Ratio	$\ u_2 - u_{2,n}\ _\infty$	Ratio
1	8	1.53E-2		1.12E-2	
2	32	1.43E-3	10.7	2.72E-3	4.1
3	128	9.50E-5	15.1	2.51E-4	10.8
4	512	6.02E-6	15.7	1.62E-5	15.5

TABLE 2. Maximum errors on surface S#2.

n	N_n	$\ u_1 - u_{1,n}\ _\infty$	Ratio	$\ u_2 - u_{2,n}\ _\infty$	Ratio
1	8	6.56E-2		6.64E-2	
2	32	5.33E-3	12.3	4.75E-3	14.0
3	128	8.66E-4	6.2	1.35E-3	3.5
4	512	1.10E-4	7.9	1.98E-4	6.8

We give results for the surface S#2. The initial triangulation of S #2 consists of eight triangular elements. Each of these elements is a portion of the surface with one octant. The Neumann data f was chosen from (6.1). In Table 2, the asymptotic pattern for the maximum error at the node points appears to be $O(\hat{\delta}_n^3)$; and to check in more detail whether the error is truly $O(\hat{\delta}_n^3)$ or $O(\hat{\delta}_n^4)$, Tables 3 and 4 give the errors for $u_{1,n}$ and $u_{2,n}$ at a representative sampling of the 18 nodes used in the coarsest triangulation of S (for $n = 1$),

$$\begin{aligned}
 v_1 &= (0, 0, 1.24), & v_2 &= (1.84, 0, 0), \\
 v_5 &= (0, -1.52, 0), & v_7 &= (1.5156, 0, 0.7578), \\
 v_8 &= (1.2621, 1.2621, 0), & v_{12} &= (-1.1421, -1.1421, 0), \\
 v_{13} &= (0, -1.3849, 0.6925), & v_{15} &= (1.6356, 0, -0.8178), \\
 v_{18} &= (0, -1.5049, -0.7525)
 \end{aligned}$$

TABLE 3. Errors at representative v_i on S#2, for $u = u_1$.

i	E_1	E_2	E_3	E_4
1	-2.51E-2	-5.02E-3	-4.73E-4	-3.41E-5
2	-4.09E-2	-4.18E-3	-2.79E-4	-1.78E-5
5	-6.56E-2	-5.33E-3	-3.27E-4	-2.24E-5
7	-3.11E-2	-2.96E-3	-7.80E-5	1.31E-5
8	-3.20E-2	-4.44E-3	-3.77E-4	-2.62E-5
12	-3.27E-2	-5.23E-3	-4.59E-4	-3.35E-5
13	-2.91E-2	-3.01E-3	-1.48E-4	2.91E-6
15	-2.65E-2	-2.39E-3	-7.59E-5	9.22E-6
18	-2.21E-2	-2.38E-3	-1.49E-4	-2.97E-6
i	$ E_1/E_2 $	$ E_2/E_3 $	$ E_3/E_4 $	
1	5.0	10.6	15.1	
2	9.8	15.0	15.7	
5	12.3	16.3	14.6	
7	10.5	37.9	6.0	
8	7.2	11.8	14.3	
12	6.3	11.3	13.7	
13	9.7	20.3	50.9	
15	11.1	31.5	8.2	
18	9.3	16.0	50.1	

along with the ratios by which these errors decrease, respectively. The subscripts refer to the indexing of node points used in our triangulation package. When looking at the individual errors, there is a pattern of an $O(\delta_n^4)$ rate of convergence at a large number of the points.

TABLE 4. Errors at representative v_i on S#2, for $u = u_2$.

i	E_1	E_2	E_3	E_4
1	-4.28E-2	-8.06E-4	1.77E-4	1.42E-5
2	-4.75E-2	-4.62E-3	-4.63E-4	-3.24E-5
5	-4.45E-2	-2.10E-4	-1.30E-4	-1.40E-5
7	-5.75E-2	-3.17E-3	-3.53E-4	-1.79E-5
8	-6.61E-2	-3.96E-3	-4.67E-4	-2.86E-5
12	-2.73E-2	-3.84E-4	-1.87E-4	-2.09E-5
13	-4.53E-2	1.03E-4	-1.27E-4	-1.97E-5
15	-5.08E-2	-2.31E-3	-3.24E-4	-2.04E-5
18	-3.98E-2	2.81E-4	-1.11E-4	-1.90E-5
i	$ E_1/E_2 $	$ E_2/E_3 $	$ E_3/E_4 $	
1	53.1	4.6	12.5	
2	10.3	10.0	14.3	
5	211.9	1.6	9.3	
7	18.1	9.0	19.7	
8	16.7	8.5	16.3	
12	71.1	2.1	8.9	
13	439.8	0.8	6.4	
15	22.0	7.1	15.9	
18	141.6	2.5	5.8	

Acknowledgments. I am grateful to K. Atkinson for helpful discussion and his interest in this problem.

REFERENCES

1. K. Atkinson, *A survey of numerical methods for the solution of Fredholm integral equations of the second kind*, SIAM Publications, Philadelphia, 1976.
2. ———, *Piecewise polynomial collocation for boundary integral equations on surfaces in three dimensions*, *J. Integral Equations* **9** (1985), 25–48.
3. ———, *Solving integral equations on surfaces in space*, in *Constructive methods for the practical treatment of integral equations* (G. Hämmerlin and K. Hoffman, eds.), Birkhäuser, Basel, 1985.

4. ———, *An introduction to numerical analysis*, 2nd ed., John Wiley and Sons, New York, 1989.
5. ———, *An empirical study of the numerical solution of integral equations on surfaces in \mathbf{R}^3* , Report on Computational Mathematics, #1, Dept. Mathematics, University of Iowa, Iowa City, 1989.
6. ———, *A survey of boundary integral equation methods for the numerical solution of Laplace's equation in three dimensions*, in *Numerical solution of integral equations* (M. Golberg, ed.), Plenum Press, New York, 1990.
7. ———, *User's guide to a boundary element package for solving integral equations on piecewise smooth surfaces*, Reports on Computational Mathematics, #44, Dept. Mathematics, University of Iowa, Iowa City, 1993.
8. K. Atkinson and D. Chien, *Piecewise polynomial collocation for boundary integral equations*, SIAM J. Sci. Statist. Comput., to appear.
9. D. Chien, *Piecewise polynomial collocation for integral equations on surfaces in three dimensions*, Ph.D. thesis, University of Iowa, Iowa City, Iowa, 1991.
10. ———, *Piecewise polynomial collocation for integral equations with a smooth kernel on surfaces in three dimensions*, J. Integral Equations Appl. **5** (1993), 315–344.
11. M. Duffy, *Quadrature over a pyramid or cube of integrands with a singularity at the vertex*, SIAM J. Numer. Anal. **19** (1982), 1260–1262.
12. G. Fairweather, F. Rizzo and D. Shippy, *Computation of double integrals in the boundary integral method*, in *Advances in computer methods for partial differential equations III* (R. Vichnevetsky and R. Stepleman, ed.), IMACS Symposium, Rutgers University, New Jersey, 1979.
13. J.L. Guermond, *Numerical quadratures for layer potentials over curved domains in \mathbf{R}^3* , SIAM J. Numer. Anal. **29** (1992), 1347–1369.
14. J.L. Guermond and S. Fontaine, *A discontinuous h - p Galerkin approximation of potential flows*, La Rech. Aéro. **4** (1991), 37–49.
15. J. Jaswon and G. Symm, *Integral equation methods in potential theory and elastostatics*, Academic Press, Boston, 1977.
16. C. Johnson and L. Scott, *An analysis of quadrature errors in second-kind boundary integral equations*, SIAM J. Numer. Anal. **26** (1989), 1356–1382.
17. R. Kress, *Linear integral equations*, Springer-Verlag, Berlin, 1989.
18. J. Lyness, *An error functional expansion for n -dimensional quadrature with an integrand function singular at a point*, Math. Comp. **30** (1976), 1–23.
19. ———, *Extrapolation-based boundary element quadrature*, Rend. Semin. Mat., Torino, to appear.
20. M. Lynn and W. Timlake, *The numerical solution of singular integral equations of potential theory*, Numer. Math. **11** (1968), 77–98.
21. S. Mikhlin, *Mathematical physics: An advanced course*, North-Holland, Amsterdam, 1970.
22. A. Rathsfeld, *On the stability of quadrature methods for the double layer potential equation over the boundary of a polyhedron*, Preprint P-math-09/91, Karl-Weierstrass-Institut für Mathematik, 1991.

- 23.** ———, *Nyström's method and iterative solvers for the solution of the double layer potential equation over polyhedral boundaries*, to appear.
- 24.** C. Schwab and W. Wendland, *On numerical cubatures of singular surface integrals in boundary element methods*, *Numerische Math.* **62** (1992), 343–369.
- 25.** R. Wait, *Use of finite elements in multidimensional problems in practice*, in *Numerical solution of integral equations* (L. Delves and J. Wallsh, ed.), Clarendon Press, Oxford, 1974.
- 26.** W. Wendland, *Asymptotic accuracy and convergence for point collocation method*, in *Topics in boundary element research, Vol. 2: Time-dependent and vibration problems* (C. Brebbia, ed.), Springer-Verlag, Berlin, 1992.
- 27.** Y. Yang, *Numerical integration for layer potentials over surfaces in \mathbf{R}^3* , submitted for publication.
- 28.** Y. Yang and K. Atkinson, *Two dimensional quadrature for functions with a point singularity on a triangular region*, *SIAM J. Numer. Anal.*, to appear.

DEPARTMENT OF MATHEMATICS, THE STATE UNIVERSITY OF NEW YORK
—FARMINGDALE, FARMINGDALE, NY 11735